Theor Chem Acc (2001) 105:431–436
DOI 10.1007/s002140000245

Theoretical
Chemistry Accounts

Regular article

Möbius strip versus linear and cyclic polyacenes: a Hückel and semiempirical investigation

Maxime Guillaume, Benoît Champagne, Eric A. Perpète, Jean-Marie André

Facultés Universitaires Notre-Dame de la Paix, Laboratoire de Chimie Théorique Appliquée, 61 rue de Bruxelles, 5000 Namur, Belgium

Received: 20 September 2000 / Accepted: 21 September 2000 / Published online: 28 February 2001

Abstract. The electronic structure of finite and infinite linear, cyclic and Möbius strip polyacenes has been investigated by adopting Hückel and semiempirical schemes. Using the Hückel approach, it turns out that the Möbius belting process modifies the highest occupied molecular orbital (HOMO)–lowest unoccupied molecular orbital (LUMO) gap in such a way its evolution with chain length is similar to the linear polyacenes rather than their cyclic analogs. These results are corroborated at the Austin model 1 (AM1) level, where the geometry relaxation effects are taken into account. The optimized AM1 structures show that the Möbius defect is localized and extends over a third of the ring. With respect to the Hückel approach, accounting for geometry distortion at the AM1 levels results in an increase in the HOMO–LUMO gap of the Möbius strip relative to the linear and cyclic finite-size structures. On the other hand, when including electron-hole correlation at the configuration interaction singles/Zerner's intermediate neglect of differential overlap level the behavior with system size of the first excitation energy of cyclic and Möbius polyacenes differs from their linear analogs and leads to smaller singlet excitation energies.

Key words: Polyacenes – Möbius strip – Austin Model 1 – Energy gap

1 Introduction

This work is a part of our long-lasting interest in the quantum chemistry of large oligomeric and polymeric species. It studies linear polyacenes (class I) made up of laterally fused benzenoid hydrocarbons, their corresponding cyclically belt structures (class II, sometimes referred to as cyclacenes [1]) as well as Möbius belt-type (class III) molecules (Fig. 1). On the one hand, polyacenes and their Möbius strips are novel, intellectually appealing molecular architectures, whereas, on the other hand, these molecules exhibit a renewed interest owing to their close similarity to short carbon nanotubes.

In this article, we investigate the topology-related differences in the electronic properties between alternant (class I and II) and nonalternant (Möbius-like, class III) hydrocarbons. Here the term alternant refers to the topology and means that the atoms of a molecule can be divided in two sets; the atoms of a given set having only atoms of the other set as neighbors. Going from the alternant to the homologous nonalternant structures has been shown to modify the mathematical properties of the solution and often to result in geometrical modifications and local charge transfers [2]. This topological alternation should, however, be distinguished from the bond length alternation (BLA) and connected electronic density alternation of which the effects are also addressed in this article. The Möbius belting procedure transforms two (one up and one down) faces into a single continuous face and destroys the intrinsic antisymmetry of the π orbitals with respect to the molecular plane.

In the first part, results are reported in the framework of the Hückel model, which has turned out to be efficient to rationalize novel concepts in domains as different as conducting polymers or nonlinear optics [3–5]. Hückel-like polymer band structures of the regular linear polyacenes were reported some 30 years ago [6]. We use the cyclic Born–Kárman boundary conditions to obtain the molecular orbitals (MOs) of oligomers from the band structures [7]. Then, orbital levels, including the highest occupied MO (HOMO) and the lowest unoccupied MO (LUMO), and energy gaps are analyzed and rationalized with respect to the size of the molecules for the three classes of systems. In particular, the HOMO–LUMO gap has been considered because it plays an important role in electric and optical properties as well as in UV/vis spectra and chemical reactions.

In the second part, a step towards reality is made by testing, in the three classes of compounds, the BLA effect as well as its associated density alternations on the energy gap.

Correspondence to: M. Guillaume

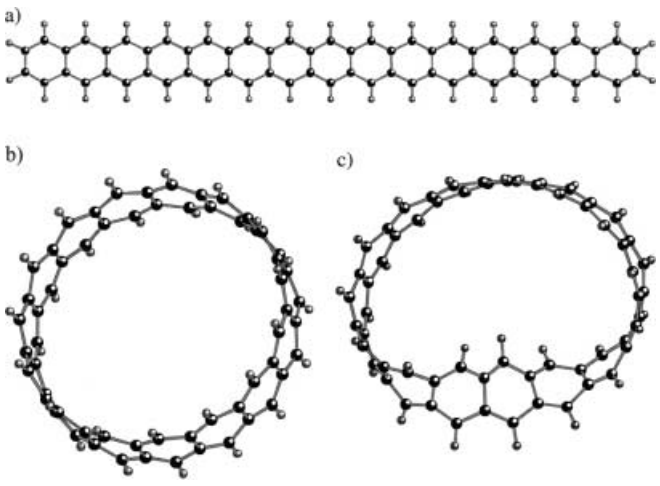

Fig. 1. Representation of the structures of the **a** linear, **b** cyclic and **c** Möbius strip polyacenes

Finally, the semiempirical Austin model 1 (AM1) technique is used to characterize the geometrical defects associated with the Möbius strips in comparison with their linear and cyclic analogs. The HOMO–LUMO AM1 energy gaps are compared to the Hückel values as well as to the lowest configuration interaction singles (CIS)/ Zerner's intermediate neglect of differential overlap (ZINDO) excitation energies. The possible interest of the three classes of molecules is examined in the light of these results.

2 Topological properties of various regular polyacenic models as investigated by simple Hückel methodology

The structures of linear, cyclic and Möbius strip polyacenes are represented in Fig. 1. The linear chains consist of $2(2N + 1)$ atom chains made up of N rings whereas the cyclic polyacenes contain N rings and $2(2N)$ carbon atoms. Class I (II) systems can also be viewed as two fused polyacetylene chains (trannulenes). The $4N$ carbon atom Möbius strips (class III) form N twisted rings. Alternatively, they can be viewed as a $2N$ unit cell polyacetylene chain of which half of the carbon atoms interacts with another site in a way to form a perfectly regular structure. The next paragraph provides the band structures for these infinite periodic and regular structures as well as their oligomeric analogs.

2.1 Linear and cyclic polyacenes

The electronic structure of the infinite polyacenic systems can be obtained from band structure calculations [3, 7–9]. The use of the Born–Kárman cyclic boundary conditions to derive the band structure implies equivalent solutions for the linear and cyclic structures. Using the techniques of polymer quantum chemistry including the Bloch theorem, we have to solve the secular determinant to get the expressions of the four π bands,

$$\begin{vmatrix} \alpha-\varepsilon & \beta(1+e^{ika}) & 0 & 0 \\ \beta(1+e^{-ika}) & \alpha-\varepsilon & \beta & 0 \\ 0 & \beta & \alpha-\varepsilon & \beta(1+e^{ika}) \\ 0 & 0 & \beta(1+e^{-ika}) & \alpha-\varepsilon \end{vmatrix} = 0 \ , \tag{1}$$

which gives the following analytic solutions:

$$\varepsilon_n(k) = \alpha \pm \beta \frac{1 \pm \sqrt{9 + 8\cos(ka)}}{2} \ , \tag{2}$$

where α and β stand for the well-known Hückel Coulomb and resonance integrals, respectively. a is the unit cell length. k belongs to the first Brillouin zone $[-\pi/a, \pi/a]$ and, using the Born–Kárman conditions, can take the values $2n\pi/Na$, with N tending to infinity. In $k = \pi/a$ (Γ) one obtains the degeneracy between the highest valence band and the lowest conduction band characterizing conducting systems. The method of finite differences [7] is one successful way to obtain the energy levels of the finite oligomeric systems according to their size. The other technique that we have adopted here consists in using the band structure expressions where the k values are properly discretized. For a linear polyacene containing N unit cells, in addition to $\alpha \pm \beta$, the electronic levels (as well as the coefficients of the linear combination of atomic orbitals) are obtained by setting

$$ka = \frac{n\pi}{N+1} \quad \text{with} \quad n = 1, 2, \ldots, N \ , \tag{3}$$

whereas for the cyclically belt structures

$$ka = \frac{2n\pi}{N} \quad \text{with} \quad n = 0, 1, 2, \ldots, N-1 \ . \tag{4}$$

These relationships between the oligomeric and polymeric electronic structures have been advantageously used by Cui et al. [10] in the reverse way, i.e. to extract polymer properties from oligomer calculations. By combining Eq. (2) with Eqs. (3) and (4) we have determined the HOMO–LUMO gap for the linear

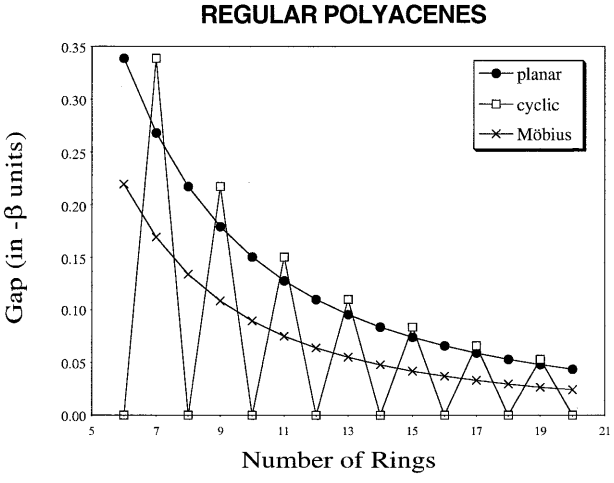

Fig. 2. Evolution with the number of rings of the highest occupied molecular orbital (*HOMO*)–lowest unoccupied molecular orbital (*LUMO*) gap for the three classes of regular bond length alternation (BLA) (=0) polyacenes obtained at the Hückel level

and cyclic polyacenes as a function of the number of rings (Fig. 2). When cyclic structures contain an even number of fused rings, the HOMO and LUMO are degenerate and the gap is zero. When the number of rings is odd, the HOMO and LUMO levels are distinct, so the gap of finite cyclic polyacenes is nonzero. This conductor/semiconductor alternation is related to the well-known Hückel $4n$ and $4n+2$ rules. In the infinite-chain limit, the even and odd cyclic structures as well as the linear polyacenes have a zero band gap. For a given number of rings, the gap of odd-numbered cyclic polyacenes is slightly larger than for their linear analogs.

2.2 Möbius strip polyacenes

To obtain the analytical band structure solution for Möbius strip polyacenes, one way is to note that, owing to the Möbius belting process, the system is built from a single strand of $2N$ unit cells containing two carbon atoms. The two carbons are linked to the two neighboring unit cells along the chain, but one of these atoms is also linked to another carbon atom N unit cells distant along the strand. Following the same approach as earlier we obtain the secular determinant

$$\begin{vmatrix} \alpha-\varepsilon & \beta\left(1+\mathrm{e}^{-ika}\right) \\ \beta\left(1+\mathrm{e}^{ika}\right) & \alpha-\varepsilon+\beta\mathrm{e}^{iNka} \end{vmatrix} = 0 \ , \tag{5}$$

which, after using the Born–Kárman cyclic boundary conditions ($ka = n\pi/N$) provides analytic solutions for the two π bands:

$$\varepsilon_n(k) = \alpha + \beta\frac{(-1)^n \pm \sqrt{9+8\cos(ka)}}{2} \ . \tag{6}$$

Comparing the later equation with Eq. (2) demonstrates that the band structures are equivalent for the three classes of polyacenes; the $(-1)^n$ factor being responsible for doubling the number of bands from 2 to 4 in the Möbius case. On the other hand, the discretization and the oligomeric results thereof are different. For the Möbius strips the first Brillouin zone is discretized according to

$$ka = \tfrac{n\pi}{N} \quad \text{with} \quad n = 0,\ 1,\ 2,\ \ldots,\ 2N-1 \ . \tag{7}$$

From the previous formulas, it is straightforward to deduce the energy of the most meaningful orbitals and the bandwidths of importance for any finite size system. The $(-1)^n$ factor is found to lift the symmetry of the MO levels with respect to the nonbonding α root. The size dependence of the HOMO–LUMO gap is displayed in Fig. 2. In the infinite-chain-length limit, the regular (from the point of view of the bond lengths and density) Möbius strips also display conducting behavior. With respect to the linear and cyclic (N odd) structures, the oligomeric gaps are smaller for an equivalent number of rings as a consequence of the doubling of the length of the conjugated chain. Indeed, in the topology language, the cyclic and linear structures belong to the nonalternant hydrocarbons whereas the Möbius strips are alternant [2].

3 Bond length alternation effects upon the electronic properties of polyacenic models as investigated by simple Hückel methodology

With the exception of the extremities of the linear polyacenes exhibiting small end effects, for the three classes of regular compounds, all unit cells are equivalent on the basis of their bond indices and charge distributions. Moreover, the CC bonds connecting these polyacetylene chains/trannulenes present a smaller π-bonding character. Anticipating the results of the semiempirical calculations, there is a second alternation along the polyacetylene chains which accounts for Peierls distortion in infinite, one-dimensional metallic chains. This distortion is known to give rise to a degeneracy lift and to the opening of the band gap. Both types of BLA effects have been modeled at the Hückel level by assigning β, β', and β'' resonance integrals, respectively, to the stronger and the weaker π bonds of the chains and to the interchain bonds. Using β as the reference, the following ratios have been defined:

$$0 \le \frac{\beta'}{\beta} = A \le 1 \ , \tag{8}$$

$$0 \le \frac{\beta''}{\beta} = B \le 1 \ . \tag{9}$$

The generalization to bond length alternant structures of the π-band expressions given in Eqs. (2) and (6) are

$$\varepsilon_n(k) = \alpha \pm \frac{\beta'' \pm \sqrt{4\beta^2 + 4\beta'^2 + \beta''^2 + 8\beta\beta'\cos(ka)}}{2} \tag{10}$$

for planar and cyclic structures and

$$\varepsilon_n(k) = \alpha + \frac{\beta''(-1)^n \pm \sqrt{4\beta^2 + 4\beta'^2 + \beta''^2 + 8\beta\beta'\cos(ka)}}{2} \tag{11}$$

for the Möbius strips. These expressions also provide the electronic levels of any finite system by following the Brillouin zone discretization procedure described in Sect. 2. Again, the discretization of the first Brillouin zone leads to differences for the three polyacene classes, whereas the band structures of the ideal infinite systems are identical. The HOMO and LUMO expressions for the various polyacenic structures are summarized in Table 1. In order to exemplify the BLA effects, values of $A = 0.935$ and $B = 0.909$ were chosen. They were obtained by injecting the AM1-optimized bond length values into [11]

$$\beta(\mathrm{eV}) = -2.40 + 3.21\left[R(\text{Å}) - 1.397\right] \ . \tag{12}$$

The effects of BLA upon the HOMO–LUMO gap are displayed in Fig. 3 for the linear, cyclic and Möbius strip polyacenes as a function of the system size. It appears that the chain-length dependence of the gap is qualitatively similar for the bond length alternant and regular systems but that the gaps of the former tend, in the infinite-chain limit, towards a finite, nonzero value:

Table 1. Analytical expressions of the highest occupied molecular orbital (*HOMO*) and lowest unoccupied molecular orbital (*LUMO*) levels of the various finite (*N* fused rings) polyacenic systems with account of bond alternations. The values are given in units of -β by taking α as the energy origin

	HOMO	LUMO
Linear	$-\frac{B-2\sqrt{1+A^2+(B/2)^2+2A\cos\left(\frac{N\pi}{N+1}\right)}}{2}$	$\frac{B-2\sqrt{1+A^2+(B/2)^2+2A\cos\left(\frac{N\pi}{N+1}\right)}}{2}$
Cyclic	Odd	
	$-\frac{B-2\sqrt{1+A^2+(B/2)^2+2A\cos\left(\frac{(N\pm1)\pi}{N}\right)}}{2}$	$\frac{B-2\sqrt{1+A^2+(B/2)^2+2A\cos\left(\frac{(N\pm1)\pi}{N}\right)}}{2}$
Even	$-\frac{B-2\sqrt{(1-A)^2+(B/2)^2}}{2}$	$\frac{B-2\sqrt{(1-A)^2+(B/2)^2}}{2}$
Möbius	Odd	
	$-\frac{B-2\sqrt{1+A^2+(B/2)^2+2A\cos\left(\frac{(N\pm1)\pi}{N}\right)}}{2}$	$\frac{B-2\sqrt{(1-A)^2+(B/2)^2}}{2}$
Even	$-\frac{B-2\sqrt{(1-A)^2+(B/2)^2}}{2}$	$\frac{B-2\sqrt{1+A^2+(B/2)^2+2A\cos\left(\frac{(N\pm1)\pi}{N}\right)}}{2}$

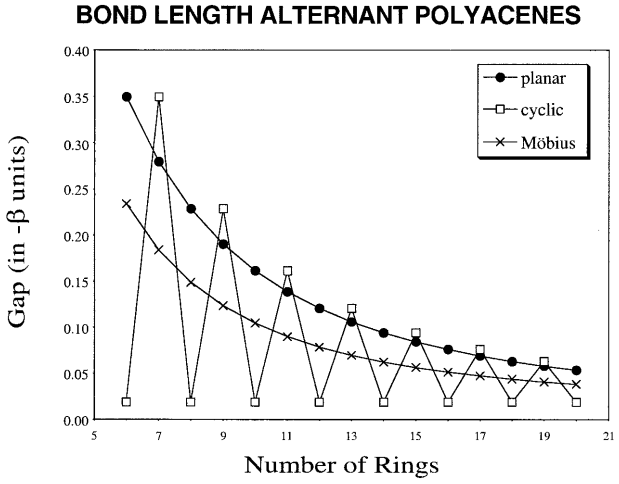

Fig. 3. Evolution with the number of rings of the HOMO–LUMO gap for the three classes of alternant polyacenes obtained at the Hückel level

$$\Delta E_g(N=\infty)=\beta\left[B-2\sqrt{(1-A)^2+(B/2)^2}\right]$$
$$\approx -2\frac{(1-A)^2}{B}=-0.0094\beta\ .$$

Again, it is interesting to note that for finite chains, the gap of the Möbius strips is smaller than for the linear polyacenes, whereas it is between the two gap values associated with the even and odd cyclic polyacene structures. The same conclusions can be drawn by using in Eqs. (10) and (11) β values corresponding to modified neglect of differential overlap (MNDO) optimized geometries. The following section adopts the AM1 semiempirical scheme and extends the characterization by considering globally the effect of the curvature of the cyclic and Möbius structures and the geometrical relaxation and possible localization of the distortion associated with the Möbius strips.

4 Towards reality: AM1 geometry optimization and CIS/ZINDO excitation energies of linear and cyclic (regular and Möbius strip) polyacenes

The AM1 scheme [12] was first employed to optimize the structure of the three classes of finite polyacenic structures, containing between six and 20 fused rings and then to analyze the geometrical effects upon the band gap given, to a first approximation, as the difference between the HOMO and LUMO levels. In a second step, the CIS/ZINDO [13] first excitation energies are computed. The inclusion of the electron-hole interactions is expected to provide improved excitation energies which can serve to simulate UV/vis spectra. These calculations were carried out using the GAUSSIAN98 program [14].

The class II oligomers display a regular structure with, for sufficiently large systems, bond length values of 1.377 and 1.431 Å along the two interacting trannulenes, whereas the distance between them amounts to 1.452 Å.

As shown in Fig. 4 by the sketch of the BLA along the chain, the planar oligomers exhibit a totally different geometry:

1. For odd oligomers, going from one extremity towards the chain center, the BLA value strongly decreases, attains zero, then reverses sign and finally increases towards the other extremity.
2. For even oligomers, the behavior is similar, with the exception that there are no identical consecutive bonds at the center of the chain and the BLA jumps from $-\delta$ to $+\delta$ with $\delta \sim 0.03$ Å.
3. When the oligomer is sufficiently large there is a region where the BLA is stable and similar to the value of the cyclically-belt structures (1.372–1.379 and 1.427–1.434 Å).
4. Border effects are associated with larger BLA. The sign reversal of the BLA is similar to the one encountered in polyacetylene chains bearing a soliton defect [15]. This coexistence of undistorted and Peierls-distorted regions is in agreement with the conclusions drawn by Cioslowski [16] from correlated ab initio results.

AM1 full geometry optimization of the Möbius strips shows that the torsion is located and extends over a third to a half of the structure. In the nondistorted region, the bond length values of the polyacetylene-type interacting chains are almost identical (1.376 and 1.432 Å) to those of the cyclic structure. For the geometrical structure in the region of the torsion-induced defect, a distinction should be made between the small (fewer than nine rings) systems and the others. For the former, the torsion is so large that it leads to bond stretchings and

contractions in such a way that one may perceive smaller and larger fused rings. For the later, the average bond length variation is much smaller and the systems maintain their six-membered fused ring structure. The evolution of the BLA along the Möbius strip containing 19 rings (38 double bonds) is displayed in Fig. 5. One sees that the defect is located around positions 10 and 30, which are facing each other, and extend over 7–8 sites. The BLA variation is larger around position 10 (~0.25 Å) than around position 30 (~0.20 Å). This larger variation is associated with the external polyacetylene chain, whereas the smaller variation is associated to the chain that points towards the cavity of the structure. In contrast to class I polyacenes, there is no sign reversal of the BLA as could have been expected from the one-chain character of the Möbius belt. Similar results were also obtained at the MNDO level.

The HOMO–LUMO gaps were evaluated for these optimized structures and are plotted in Fig. 6. Qualitatively, the AM1 results are equivalent to those obtained at the Hückel level, which neglects the σ electrons, the curvature of the cyclic and Möbius structures as well as the geometry relaxation effects associated with the Möbius belting process. However, with respect to the Hückel treatment, the HOMO–LUMO gaps of the Möbius strips increase relative to the other systems and are almost similar to the gaps of the linear and odd cyclic polyacenes. Moreover, the geometrical distortions present in the smallest Möbius strip structures do not lead to a different size dependence of the energy gap but only to a small HOMO–LUMO gap increase with respect to their linear analogs. The chain-length dependence – including parity effect – of the MNDO HOMO–LUMO results due to Türker [17] are qualitatively similar to ours; the HOMO–LUMO gap being, however, about 1.5 eV smaller than ours for the Möbius strips.

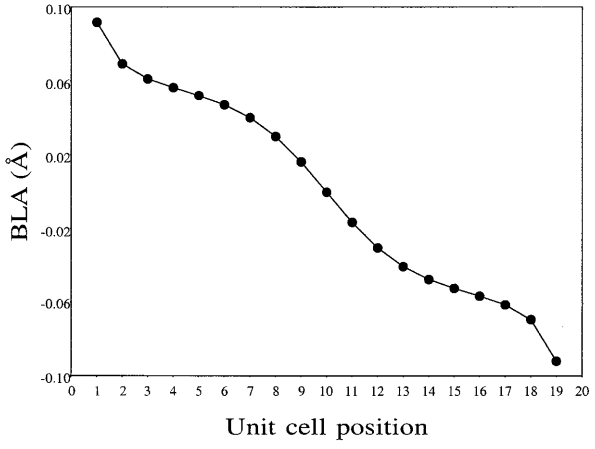

Fig. 4. Evolution of the BLA along the backbone of the linear polyacene containing 19 rings obtained at the Austin model 1 (*AM1*) level of approximation

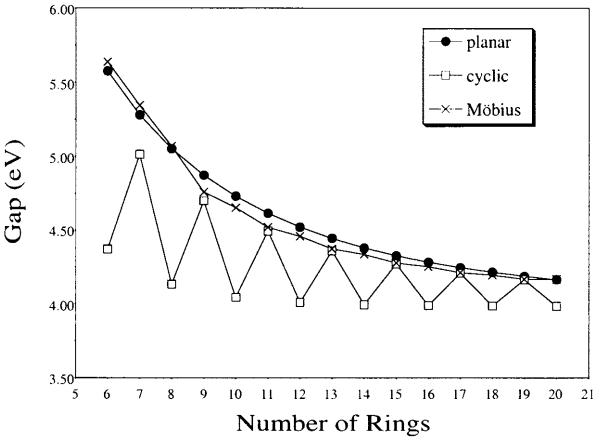

Fig. 6. Evolution with the number of rings of the HOMO–LUMO gap for the linear, cyclic and Möbius strip polyacenes obtained at the AM1 level by employing the AM1 fully optimized geometry

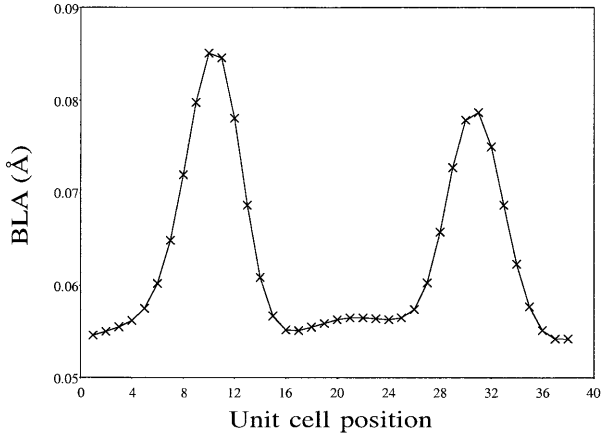

Fig. 5. Evolution of the BLA along the backbone of the Möbius strip polyacene containing 19 rings (38 carbon–carbon double bonds) obtained at the AM1 level of approximation. Note that the scale is different from that used in Fig. 4

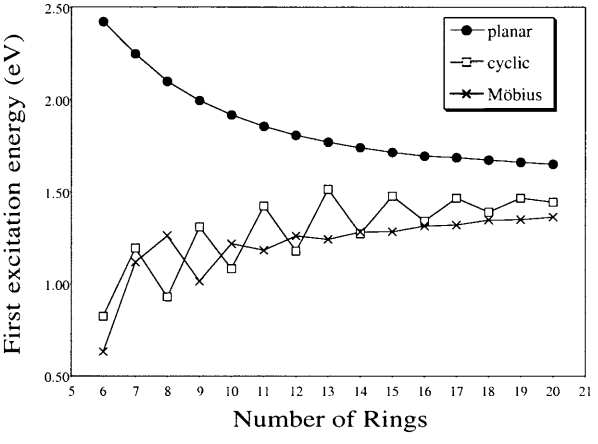

Fig. 7. Evolution with the number of rings of the first excitation energy for the linear, cyclic and Möbius strip polyacenes obtained at the configuration interaction singles/Zerner's intermediate neglect of differential overlap level by employing the AM1 fully optimized geometry

Finally, the lowest-energy singlet CIS/ZINDO excitation energies were determined and are represented versus the number of rings in Fig. 7 for the three types of polyacenes. Like the HOMO–LUMO gaps, the first excitation energy of the cyclic polyacenes displays sawtooth behavior, whereas for the planar structures, the evolution is smooth. For the Möbius strips a smaller and opposite sawtooth behavior is observed. By looking carefully at Fig. 6, this behavior was already present for the HOMO–LUMO gap, while it is magnified by the inclusion of electron-hole interactions. In contrast to the AM1 and Hückel HOMO–LUMO gaps, the first excitation energy of the cyclic and Möbius polyacenes increases with the system size. Moreover, for the three classes of compounds the excitation energy tends, in the large-system limit, to a value ranging between 1.3 and 1.7 eV, characteristic of semiconducting behavior.

5 Summary and outlook

The electronic structure of finite and infinite linear, cyclic and Möbius strip polyacenes has been investigated by adopting the Hückel and semiempirical schemes. Using the Hückel approach, it turns out that the Möbius belting process modifies the HOMO–LUMO gap in such a way that its evolution with chain length is similar to the linear polyacenes rather than their cyclic analogs. These results are corroborated at the AM1 levels, where the geometry relaxation effects are taken into account. The optimized AM1 structures show that the Möbius defect is localized and extends over a third of the ring. With respect to the Hückel approach, accounting for geometry distortion at the AM1 levels results in an increase in the gap of the Möbius strip relative to the linear and cyclic finite size structures. On the other hand, when including electron-hole correlation at the CIS/ZINDO level the behavior with system size of the first excitation energy of cyclic and Möbius polyacenes differs from their linear analogs and leads to smaller singlet excitation energies. Future aspects of interest involve addressing the spin instability problem and the magnetic properties in relation to the regularity of the BLA patterns.

Although the synthesized Möbius strips reported so far are nonconjugated compounds [18], recent studies on related systems have shown that cyclacene-based materials may exhibit interesting magnetic [2], conducting [19] and electronic [20] properties. Additional experimental and theoretical studies are therefore awaited to improve the understanding of these challenging compounds.

Acknowledgements. The authors thank O. Quinet for helping them in generating automatically the oligomeric Hückel data. B.C. and E.A.P. thank the Belgian National Fund for Scientific Research for their Research Associate and Postdoctoral Researcher positions, respectively M.G. thanks the Fonds pour la Formation à la Recherche dans l'Industrie et l'Agriculture (FRIA) for financial support. The calculations were performed using the IBM SP2 of the Namur Scientific Computing Facility. The authors gratefully acknowledge the financial support of the FNRS-FRFC and the Loterie Nationale for convention N 2.4519.97.

References

1. Choi HS, Kim KS (1999) Angew Chem Int Ed Engl 38: 2256
2. Seo DK, Hoffmann R (1999) Theor Chem Acc 102: 23
3. André JM, Delhalle J, Brédas JL (1991) Quantum chemistry aided design of organic polymers for molecular electronics. World Scientific, Singapore, pp 377
4. André JM, Champagne B (1999) In: Brédas JL (ed) Conjugated oligomers, polymers, and dendrimers: from polyacetylene to DNA. Proceedings of the Fourth Francqui Colloquium, De Boeck Université, Brussels, 1999, p 349
5. Gineityte V (1999) J Mol Struct (THEOCHEM) 491: 205
6. (a) André JM, Gouverneur L, Leroy G (1967) Int J Quantum Chem 1:427; (b) André JM, Gouverneur L, Leroy G (1967) Bull Soc Chim Belg 76: 661
7. Rebane TK (1965) In: Veselov MG (ed) Methods of quantum chemistry. Academic, New York, p 147
8. Ladik J (1988) Quantum theory of polymers as solids. Plenum, New York
9. Kertesz M (1982) Adv Quantum Chem 15: 161
10. Cui CX, Kertesz M, Jiang Y (1990) J Phys Chem 94: 5172
11. Risser S, Klemm S, Allender DW, Lee MA (1987) Mol Cryst Liq Cryst Sci Technol Sect B 150: 631
12. Dewar MJS, Zoebisch EG, Healy EF, Stewart JJP (1985) J Am Chem Soc 107: 3902
13. Ridley JE, Zerner M (1973) Theor Chim Acta 32: 111
14. Frisch MJ, Trucks GW, Schlegel HB, Scuseria GE, Robb MA, Cheeseman JR, Zakrezewski VG, Montgomery JA, Stratmann RE, Burant JC, Dapprich S, Millam JM, Daniels AD, Kudin KN, Strain MC, Farkas O, Tomasi J, Barone V, Cossi M, Cammi R, Mennucci B, Pomelli C, Adamo C, Clifford S, Ochterski J, Petersson GA, Ayala PY, Cui Q, Morokuma K, Malick DK, Rabuck AD, Raghavachari K, Foresman JB, Cioslowski J, Ortiz JV, Stefanov BB, Liu G, Liashenko AP, Piskorz AP, Komaromi I, Gomperts R, Martin RL, Fox DJ, Keith T, Al-Laham MA, Peng CY, Nanayakkara A, Gonzalez C, Challacombe M, Gill PMW, Johnson BG, Chen W, Wong MW, Andres JL, Head-Gordon M, Repolgle ES, Pople JA (1998) GAUSSIAN 98, revision A.1. Gaussian, Pittsburgh, Pa
15. Champagne B, Deumens E, Öhrn Y. (1997) J Chem Phys 107: 5433, and references therein
16. Cioslowski J (1993) J Chem Phys 98: 473
17. Türker L (1998) J Mol Struct (THEOCHEM) 454: 83
18. Walba DM, Richards RM, Haltiwanger RC (1982) J Am Chem Soc 104: 3219
19. Sabra MK (1996) Phys Rev B 53: 1269
20. Velikanov MV, Genin H, Hoffmann R (1997) Chem Mater 9: 573